Life-Cycle of Structures and Infrastructure Systems – Biondini & Frangopol (Eds)

Temperature dependent modelling approach for early age behavior of printable mortars

A. Robens-Radermacher & J.F. Unger
Modelling and Simulation, Bundesanstalt für Materialforschung und -prüfung (BAM), Berlin, Germany

A. Mezhov & W. Schmidt
Technology of Construction Materials, Bundesanstalt für Materialforschung und -prüfung (BAM), Berlin, Germany

ABSTRACT: Structural build-up describes the stability and early-age strength development of fresh mortar used in 3D printing. It is influenced by several factors, i.e. the composition of the printable material, the printing regime, and the ambient conditions. The existing modelling approaches for structural build-up usually define the model parameters for a specific material composition without considering the influence of the ambient conditions. The goal of this contribution is to explicitly include the temperature dependency in the modelling approach. Temperature changes have significant impact on the structural build-up process: an increase of the temperature leads to a faster dissolution of cement phases and accelerates hydration. The proposed extended model includes temperature dependency using the Arrhenius theory. The new model parameters are successfully calibrated based on Viskomat measurement data using Bayesian inference. Furthermore, a higher impact of the temperature in the re-flocculation as in the structuration stage is observed.

1 INTRODUCTION

For extrusion-based 3D concrete printing, the early age of printable mortars is of great importance, which is affected by various time dependent phenomena like structural build-up, plasticity as well as viscosity. Structural build-up is the time dependent structuration of cementitious material at rest due to thixotropy and early hydration processes. It influences the printability, buildability, and open time of printing processes (Reiter et al., 2018, Mohan et al., 2021). For a deeper introduction it is referred to (Roussel et al., 2012). Generally, the structural build-up is influenced by several factors from the raw material constituents to external conditions such as temperature as discussed in detail in (Jiao et al., 2021).

There are several approaches to model the structural build-up of cementitious materials. Most phenomenological models are based on a time-dependent internal structural parameter describing the flocculation state, which is assumed to be zero after mixing and increases with time (Roussel, 2006). The approaches differ in the definition of the time dependency (linear, exponential, bilinear). In the most often used model proposed by (Roussel, 2006), the static yield stress at rest increases linearly in time with the constant structuration rate A_{thix} from an initial value τ_{y_0}:

$$\tau_y(t) = \tau_{y_0} + A_{thix}\ t. \tag{1}$$

Covering the speed-up of the structural build-up after a certain time due to an onset of the acceleration period of hydration, an exponential dependency is proposed in (Perrot et al., 2015). The static yield stress following this exponential model is given as:

$$\tau_y(t) = A_{thix} t_c \left(e^{\frac{t}{t_c}} - 1\right) + \tau_{y_0}, \tag{2}$$

DOI: 10.1201/9781003323020-146

with an additional parameter of the characteristic time t_c. Recently, (Kruger et al., 2019) developed a bi-linear approach considering two stages of the structural build-up development with different rates: re-flocculation and structuration. By differentiating between those stages a higher precision of the first rapid re-flocculation stage dominated by physical processes is possible. The structuration stage is mainly governed by chemical reactions. The static yield stress according to the Kruger model is then given by two equations:

$$\tau_y(t) = \begin{cases} \tau_{y_0} + R_{thix}t & if\ t < t_{rf} \\ \tau_y(t_{rf}) + A_{thix}(t - t_{rf}) & if\ t < t_{rf} \end{cases}. \tag{3}$$

In the latter, the re-flocculation time t_{rf} defines the time period between the first stage with the re-flocculation rate R_{thix} and the second structuration stage (A_{thix}). The ratio between both rates depends on the material mixture composition (Kruger et al., 2019). In (Ivanova et al., 2022) the bilinear model is applied in the context of constant rotational velocity tests of printable mortar and concrete and for several characterization methods of 3D printable cementitious mortars in (Bos et al., 2021).

Usually, the model parameters are defined for a specific material composition without considering the influence of ambient conditions. Nevertheless, ambient conditions such as temperature and humidity will change in real life printing processes due to weather conditions, summer, winter, day, night as well as the printing process itself (pumping process changes the temperature due to pressure changes (Strangfeld, 2022)). In the discussion of eight implemented 3D concrete printing projects from around the world by (Bos et al., 2022), the challenges of the ambient temperatures' influence were also pointed out. Printings were stopped or shifted to the night by increased ambient temperature or a continuous measurement of the system temperature were applied. The temperature has a particularly significant influence on the structural build-up process because an increase of the temperature leads to a faster dissolution of cement phases and accelerates hydration. Nevertheless, there are only limited studies available to date. (Bos et al., 2019) investigated the influence of material temperature and they have shown that warm water accelerates the structural build-up rate but reduces the bonding strength between layers. (Huang et al., 2019) have shown that the increase of the temperature in a constant shear rate test of cement pastes results in an increase of the structural build-up rate. The temperature sensitivity is studied by calculating the activation energy by Arrhenius theory. They extend their studies by measuring the storage modulus by small amplitude oscillatory shear test (SAOS) in (Huang et al., 2022). It was pointed out that a rise of the temperature leads to a faster storage modulus development for cement paste samples with the same hydration degree. However, (Bogner et al., 2020) using SAOS tests at 10, 20, 25 and 30°C, found out that regardless of the ambient temperature, all investigated samples demonstrated a similar evolution of the complex shear modulus during the first 1.4 h of hydration. After that, a significant temperature influence on the modulus was observed. The discrepancy between those results could also be related to the different material compositions, methods, and time scales. The authors themselves observed a significant temperature influence on the storage moduli for cement pastes measured by SAOS with a bi-linear increase over the resting time (Mezhov et al., 2022).

The goal of this contribution is to develop a temperature dependent structural build-up model. Therefore, the bi-linear Kruger model (Equation 3) is extended by temperature dependent parameters modelled based on the Arrhenius theory. The new model parameters are estimated using Bayesian inference. Therefore, static yield stress data measured via Viskomat at four different temperature levels are used.

2 MATERIALS AND METHODS

2.1 *Mixture composition and measurement set-up*

Mortar samples were prepared according to the mixture composition given in Table 1. First cement CEM I 42.5 R, silica fume, sand, fly ash and superplasticizer were mixed with a spoon

around 30 sec in a 600 ml cup. The water was added within 15 sec during the second mixing at 200 rpm for 1 min by IKA STARVISC 200–2.5 mixer. After a pause and hand mixing for 30 sec, the mortar samples were mixed at 400 rpm for 2 min.

Table 1. Mixture composition.

Components	Amount [kg/m^3]
Cement (CEM I 42.5 R)	650
Sand (0.1/0.5)	980
Fly ash	190
Silica fume	90
Superplasticizer powder	4.3
Water	260
Spread by DIN EN 1015-3:1999-04	190 mm
Water cement ratio	0.4
Temperature after mixing	27°C

The structural build-up measurements were performed using a Schleibinger Viskomat NT with a double gab basket cell. The used device can measure torque from 0 to 500 Nmm. Note, the mixture composition was designed in such a way that the maximum torque does not exceed those range for all investigated temperature levels. Ten points with a rotational velocity of 0.1 rpm within 30 min were measured. The test protocol is summarized in Figure 1. Three tests for every temperature were carried out using a waterbed temperature control system with constant temperatures 17, 22, 27, 32 and 42°C. The initial temperature of the mortar after mixing was always 27°C.

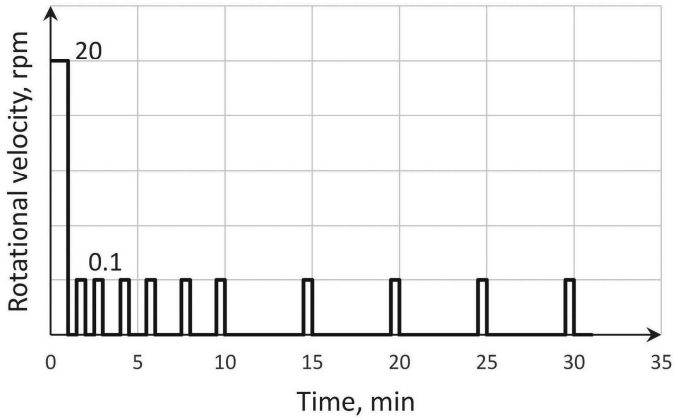

Figure 1. Test protocol for Viskomat NL measurements.

2.2 *Temperature dependent structural build-up model*

The bi-linear model of (Kruger et al., 2019) given in Equation 3 is extended to model the temperature influence on the early age behavior of the static yield stress τ_y. Therefore, the model parameters re-flocculation rate, structuration rate, re-flocculation time and initial static yield stress are introduced as temperature (T) dependent functions. So that the temperature dependent bi-linear model reads:

$$\tau_y(t,T) = \begin{cases} \tau_{y_0}(T) + R_{thix}(T)t & if\ t < t_{rf}(T) \\ \tau_y\left(t_{rf}(T),T\right) + A_{thix}(T)\ \left(t - t_{rf}\right) & if\ t > t_{rf}(T) \end{cases}. \tag{4}$$

Where the temperature dependent parameter functions are defined as:

$$\gamma(T) = \alpha_\gamma \exp\left(\beta_\gamma \left(\frac{1}{T} - \frac{1}{T_{ref}}\right)\right) \tag{5}$$

for $\gamma \in \left[\tau_{y0},\ R_{thix},\ A_{thix},\ t_{rf}\right]$. This exponential functionality of a reaction rate of chemical as well as physical processes is known as Arrhenius equation. In the Arrhenius equation, the pre-factor β_γ in Equation 5 is defined by the negative ratio of a specific activation energy E_a and the gas constant R. Among other things, the Arrhenius theory is usually applied to model and characterize the temperature dependency of the cement hydration, see e.g. (Poole et al., 2007, Carette and Staquet, 2016). The unknown activation energy is thereby usually determined by calorimetry. Here, the Arrhenius equation is used to consider the temperature dependency of the structural build-up rates (re-flocculation rate and structuration rate) as well as for the re-flocculation time and the initial yield stress. The extended temperature dependent bi-linear model in Equation 4 and 5 has in total nine new unknown model parameters: the four α's and β's and the reference temperature T_{ref}. Those are to be defined via measurement data at different ambient temperatures for each mixture composition.

2.3 *Bayesian model parameter estimation*

In general, the estimation of unknown model parameters based on measured data is an inverse problem. The aim is to find appropriate values for a set of unknown model parameters $\boldsymbol{\theta}$ (here the model parameters in Equation 4 and 5) minimizing the error between a given set of measurement data $\boldsymbol{y}$ and the corresponding model output values $\boldsymbol{g}(\boldsymbol{\theta})$ (here Equation 4). In deterministic methods, the best parameter set is found by minimizing this difference by optimization approaches e.g. least-squares, L_p norm or weighted least square ansatz (see e.g. (Mohammad-Djafari, 1998)). The solution is a single set of the parameters' estimates and carry no information about how reliable or likely they are. In contrast, probabilistic methods provide a probabilistic description of information and beliefs, allowing the consideration of various uncertainties. In those approaches, the posterior probability distribution is computed using the Bayes' rule via

$$P(\boldsymbol{\Theta}|\boldsymbol{y}) = \frac{P(\boldsymbol{y}|\boldsymbol{\Theta})P(\boldsymbol{\Theta})}{\int P(\boldsymbol{y}|\boldsymbol{\Theta})p(\boldsymbol{\Theta})d\boldsymbol{\Theta}}. \tag{6}$$

In the latter, the unknown parameter vector $\boldsymbol{\Theta} = (\boldsymbol{\theta}, \sigma)$ includes beside the model parameters $\boldsymbol{\theta}$ additional noise parameters σ (describing e.g. the standard deviation of a Gaussian distributed additive noise $e \sim N(0, \sigma^2)$). The prior probability density function $P(\boldsymbol{\Theta})$ reflects the prior knowledge on the parameters, while the likelihood $P(y|\boldsymbol{\Theta})$ defines the probability that the model has generated the data under the given model parameters. The normalization term in the denominator describes the evidence for the data considering the model. More details on the mathematical background can be found e.g. in (Watanabe, 2018).

The computation of the posteriori (Equation 6) is cumbersome, especially with increasing dimensionality of the parameter space. For that reason, sampling-based methods (Lye et al., 2020) are usually applied to evaluate Equation 6. In this paper, the well-known Markov Chain Monte Carlo (MCMC) sampling (Metropolis et al., 1953) is used. The parameter estimation is conducted via the open-source Python package *probeye (https://pypi.org/project/probeye/)*.

3 RESULTS AND DISCUSSION

The measured temperature effect on the static yield stress evaluation in the first 30 minutes is given in Figure 2. The mean and standard deviation of the static yield stress based on three tests (stars) for all investigated temperature levels are given over the time as solid line and bars, respectively. The static yield stress is computed from the measured torque multiplied by the conversion factor for the specific cell. Two aspects are shown. First, a significant temperature effect in the yield stress evaluation is observed. With increasing ambient temperature, the rate of the static yield stress evolution increases confirming the need of a temperature dependent modelling approach. Second, the evaluation is split into two stages: a re-flocculation stage followed by

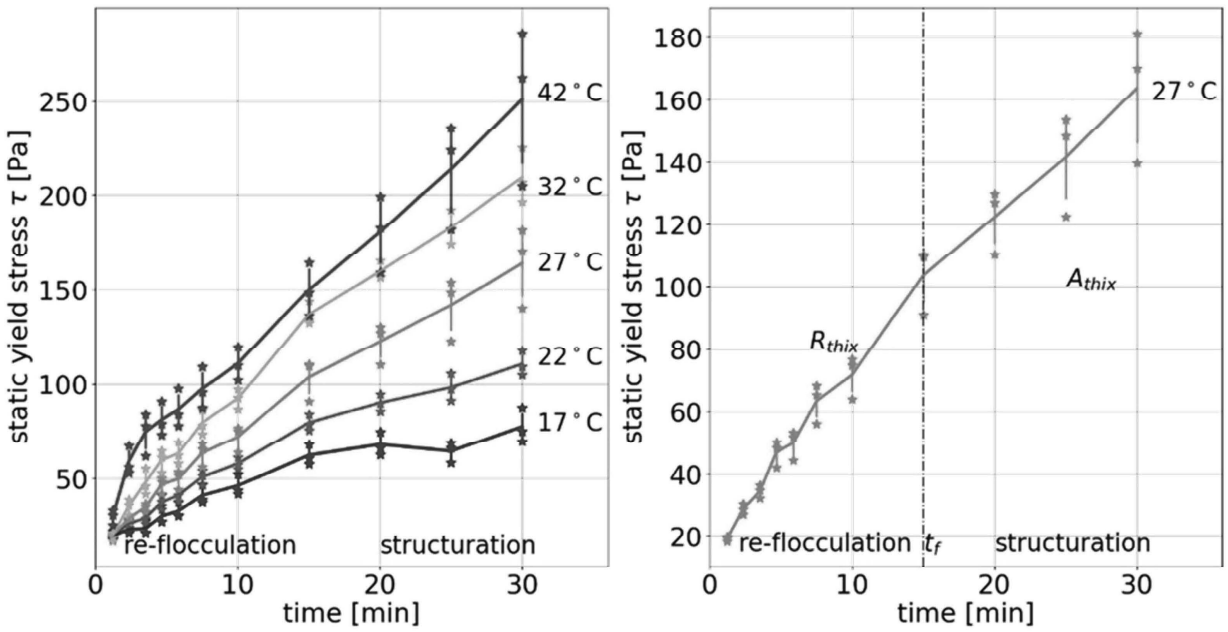

Figure 2. Mean and standard deviation of static yield stress measurements over time for five different temperatures. Separation into re-flocculation and structuration stage demonstrated for the data at 27 °C.

a structuration stage which is additional demonstrated using the data at 27°C on the right side of Figure 2. The change between the two stages, the re-flocculation time, happens around 15 min. Independent of the ambient temperature, the first (re-flocculation) rate is usually higher than the second (structuration) rate. The rate's ratio depends on the temperature.

In a Bayesian parameter estimation, the model parameters of the proposed temperature dependent model were inferred using the measured data at temperature 17, 22, 27 and 42°C (the data at $T = 32°C$ is used for the verification). Therefore, a MCMC solver with 10^6 steps in 20 chains and 5000 initial steps were running using the open-source Python module *probeye*. The prior distribution for the nine model parameters were chosen as:

$$\alpha_{\tau_{y_0}} \sim N(20,\ 6^2)\ [\text{Pa}],\ \alpha_{R_{thix}} \sim N(6,\ 2^2)\ [\text{Pa/min}],\ \alpha_{A_{thix}} \sim N(4,\ 1^2)\ [\text{Pa/min}],\ \alpha_{t_{rf}} \sim N(10,\ 3^2)\ [\text{min}]$$
$$\beta_{\tau_{y_0}} \sim N(-30,\ 9^2)\ [1/\text{K}],\ \beta_{R_{thix}} \sim N(-30,\ 9^2)\ [1/\text{K}],\ \beta_{A_{thix}} \sim N(-10,\ 3^2)\ [1/\text{K}],\ \beta_{t_{rf}} \sim N(0,\ 3^2)\ [1/\text{K}]$$
$$\sigma \sim U(1,\ 30)\ [\text{Pa}].$$

For the reference temperature, the sample's temperature after mixing was used: $T_{ref} = 27°C$.

The resulting predictive posterior probability is plotted in Figure 3 as a pair plot. Here, the advantage of using a probabilistic approach can be seen. Instead of one parameter set (like the result of a deterministic approach), the deviation and correlation of the model parameters are estimated. Especially, the parameter α_{Rthix} (in the figure α_2) and $\alpha_{\tau_{y_0}}$ (α_1) as well as $\beta_{\tau_{y_0}}$ (β_2) and $\beta_{R_{thix}}$ (β_1) are clearly correlated, showing the ill-posedness of the inverse problem. Note, the results are also influenced by the here chosen prior distributions. Furthermore, a close to zero mean of $\beta_{t_{rf}}$ (β_4) indicates a neglectable temperature dependency of the re-flocculation time. An averaged ratio between $\beta_{R_{thix}}(\beta_2)$ and $\beta_{A_{thix}}$ (β_3) of around two suggests a significant higher activation energy of the re-flocculation stage compared to the structuration stage.

The inferred temperature dependency of the primary parameters: initial yield stress τ_{y_0}, re-flocculation rate R_{thix}, structuration rate A_{thix} and re-flocculation time t_{rf}, modelled by the functionality given in Equation 5 is evaluated in Figure 4. The solid line represents the mean values, whereas the bars give the first standard deviation based on the MCMC samples. The plot visualizes the significant temperature dependency in the rates. But the structuration rate is less temperature dependent as the re-flocculation rate. The physical processes in the re-flocculation stage seems to have a higher temperature sensitivity, where rising temperatures increase the Brownian motion between the particles. Additionally, the shape of the temperature dependency of the two rates differs. The re-flocculation rate increases nearly linear, where

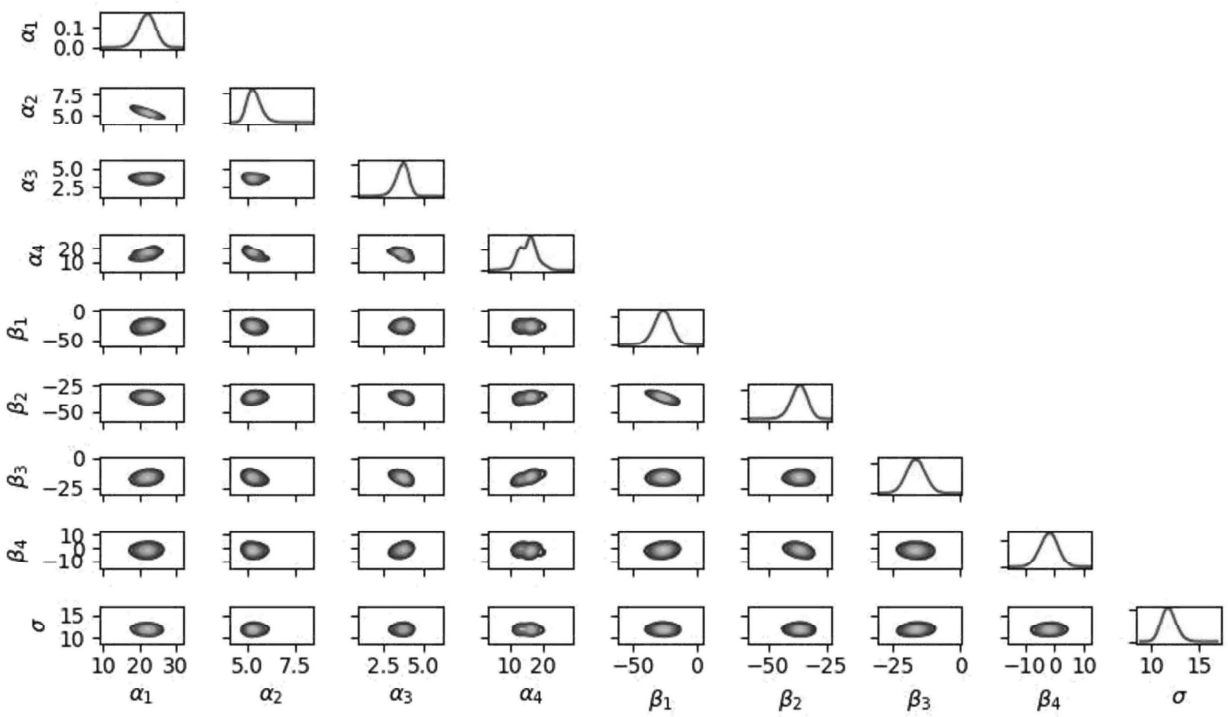

Figure 3. Pair plot of the posterior distribution with the abbreviations $1 : \tau_{y_0},\ 2 : R_{thix}, 3 : A_{thix},\ 4 :\ t_{rf}$.

the structuration rate temperature function seems to be logarithmic. Furthermore, the initial static yield stress increases like the re-flocculation rate since both parameters describe the re-flocculation stage. In contrast, the re-flocculation time is approximately independent of the temperature with an aver-aged value of around 15 min. The measurement noise was assumed to be temperature independent, and its mean is estimated as 12 Pa.

As verification of the proposed temperature dependent structural build-up model in Equation 4 and 5 the model is reevaluated for the training temperature values 17, 22, 27 and 42°C using the estimated parameter distribution as well as newly evaluated at temperature 32°C and compared to the corresponding measured data. That comparison is shown in Figure 5 given the mean model

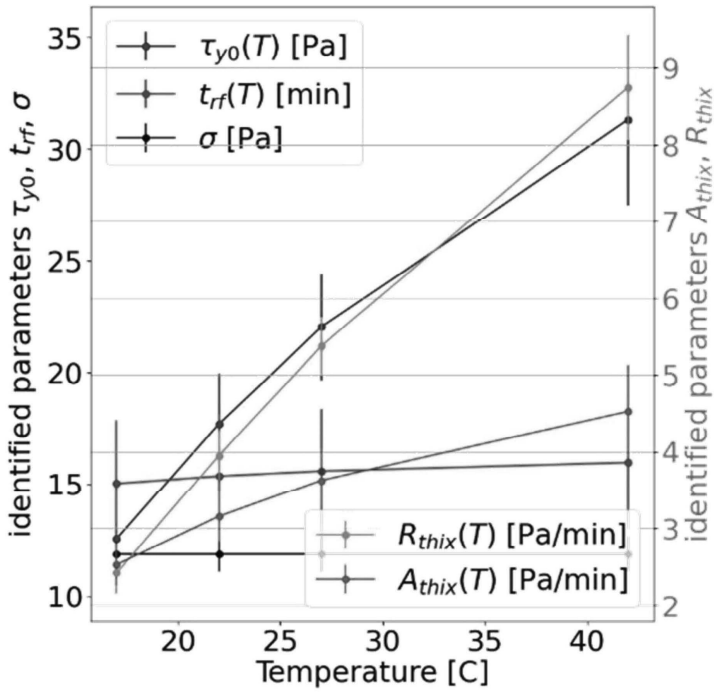

Figure 4. Inferred temperature dependency computed with Equation 6.

response as well as its first standard deviation for each temperature value and the measured data. A very good agreement for all investigated temperature values is reached even for those which were not included in the calibration part. In this way, the proposed model seems promising in predicting the temperature influence on the structural build-up of fresh mortar.

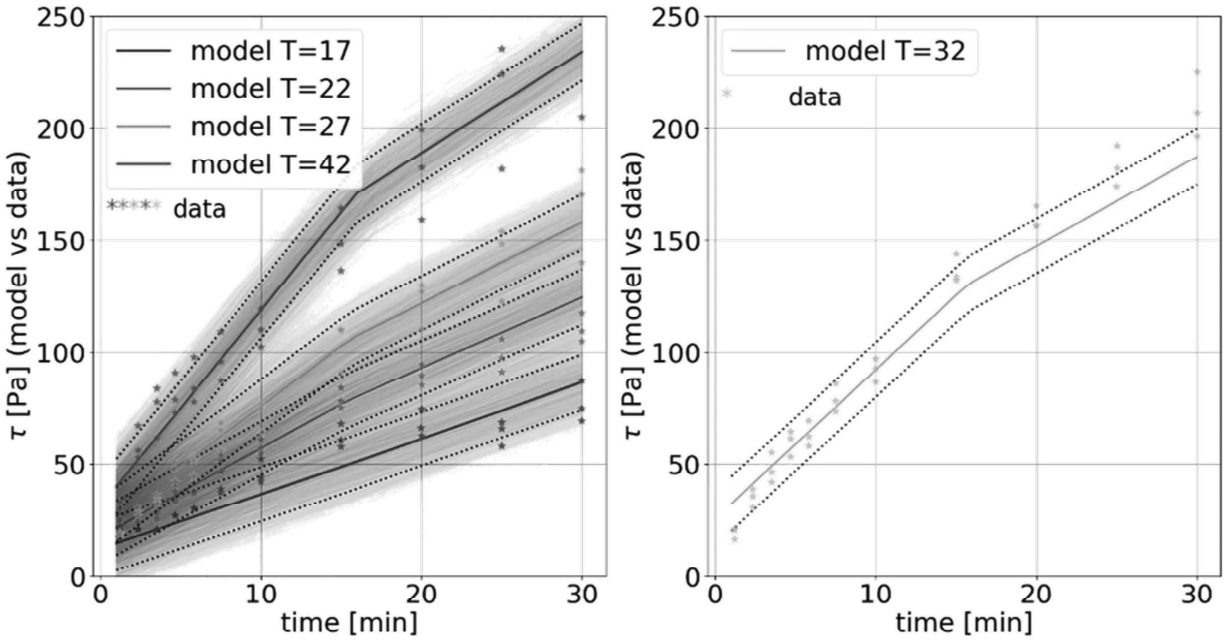

Figure 5. Inferred temperature dependency (mean as solid line and first standard deviation as dashed line of the static yield stress according to Equation 5 compared to the measured data (stars).

4 CONCLUSION

The present paper presents experimental results of the constant shear rate test indicating the influence of different ambient temperatures on the structural build-up evolution of mortar. The measured yield stress data show a presence of two stages: a re-flocculation period and a structuration stage. The temperature influence is more pronounced in the first re-flocculation stage dominated by physical processes. A new temperature dependent model approach is derived by extending the bi-linear Kruger model capturing this temperature sensitivity of the structural build-up for fresh cementitious materials. The model assumes temperature dependent functions based on the Arrhenius equation for the rates (re-flocculation and structuration rate) as well as for the initial yield stress and re-flocculation time parameters. In a Bayesian parameter estimation, the proposed model parameters are estimated for the investigated mortar composition. The analysis identifies a nearly linear temperature dependency in the re-flocculation rate, whereas the re-flocculation time is nearly temperature independent. Furthermore, a lower temperature sensitivity of the structuration rate with a logarithm shape over temperature is detected. The identified model shows very good agreement with the measured data, even for those not included in the parameter estimation process. Therefore, the proposed model could be used predicting the temperature sensitivity of structural build-up of cementitious materials. Of course, for more general conclusions further verification studies are required based on additional experimental data e.g. varying the cement type, the water content as well as using different admixtures and additions.

REFERENCES

Bogner, A., Link, J., Baum, M., Mahlbacher, M., Gil-Diaz, T., Lützenkirchen, J., Sowoidnich, T., Heberling, F., Schäfer, T., Ludwig, H.-M., Dehn, F., Müller, H.S. & Haist, M. 2020. Early hydration

and microstructure formation of Portland cement paste studied by oscillation rheology, isothermal calorimetry, 1H NMR relaxometry, conductance and SAXS. *Cement and Concrete Research* 130: 105977.
Bos, F.P., Kruger, P.J., Lucas, S.S. & van Zijl, G.P.A.G. 2021. Juxtaposing fresh material characterisation methods for buildability assessment of 3D printable cementitious mortars. *Cement and Concrete Composites* 120: 104024.
Bos, F.P., Menna, C., Pradena, M., Kreiger, E., da Silva, W.R.L., Rehman, A.U., Weger, D., Wolfs, R. J.M., Zhang, Y., Ferrara, L. & Mechtcherine, V. 2022. The realities of additively manufactured concrete structures in practice. *Cement and Concrete Research* 156: 106746.
Bos, F.P., Wolfs, R.J.M., Ahmed, Z.Y., Hermens, L.J. & Salet, T.A.M. 2019. The influence of material temperature on the in-print strength and stability of a 3D print mortar. *Advances in Engineering Materials, Structures and Systems: Innovations, Mechanics and Applications:* 425–430.
Carette, J. & Staquet, S. 2016. Monitoring and modelling the early age and hardening behaviour of eco-concrete through continuous non-destructive measurements: Part I. Hydration and apparent activation energy. *Cement and Concrete Composites* 73: 10–18.
Huang, H., Huang, T., Yuan, Q., Zhou, D., Deng, D. & Zhang, L. 2019. Temperature dependence of structural build-up and its relation with hydration kinetics of cement paste. *Construction and Building Materials* 201: 553–562.
Huang, T., Yuan, Q., Zuo, S., Yao, H., Zhang, K., Wang, Y., Xie, Y. & Shi, C. 2022. Physio-chemical effects on the temperature-dependent elasticity of cement paste during setting. *Cement and Concrete Composites* 134: 104769.
Ivanova, I., Ivaniuk, E., Bisetti, S., Nerella, V.N. & Mechtcherine, V. 2022. Comparison between methods for indirect assessment of buildability in fresh 3D printed mortar and concrete. *Cement and Concrete Research* 156: 106764.
Jiao, D., de Schryver, R., Shi, C. & de Schutter, G. 2021. Thixotropic structural build-up of cement-based materials: A state-of-the-art review. *Cement and Concrete Composites* 122: 104152.
Kruger, J., Zeranka, S. & van Zijl, G. 2019. An ab initio approach for thixotropy characterisation of (nanoparticle-infused) 3D printable concrete. *Construction and Building Materials* 224: 372–386.
Lye, A., Cicirello, A. & Patelli, E. 2020. A review of stochastic sampling methods for Bayesian inference problems. In: Zio, E & Beer, M. (eds.) *Proceedings of the 29th European Safety and Reliability Conference*. Signapore: Research Publishing.
Metropolis, N., Rosenbluth, A. W., Rosenbluth, M.N., Teller, A.H. & Teller, E. 1953. Equation of State Calculations by Fast Computing Machines. *Journal of Chemical Physics* 21: 1087–1092.
Mezhov, A., Robens-Radermacher, A., Zhang, K., Kühne, H-C., Unger, J.F. & Schmidt, W. 2022. Temperature Impact on the Structural Build-Up of Cementitious Materials – Experimental and Modelling Study. In: Buswell, R., Blanco, A., Cavalaro, S., Kinnell, P. (eds) *Third RILEM International Conference on Concrete and Digital Fabrication. DC 2022*. Loughborough: RILEM Bookseries,
Mohammad-Djafari, A. 1998. From deterministic to probabilistic approaches to solve inverse problems, In: *Proceeding SPIE 3459, Bayesian Inference for Inverse Problems*. San Diego.
Mohan, M.K., Rahul, A.V., de Schutter, G. & van Tittelboom, K. 2021. Extrusion-based concrete 3D printing from a material perspective: A state-of-the-art review. *Cement and Concrete Composites* 115: 103855.
Perrot, A., Pierre, A., Vitaloni, S. & Picandet, V. 2015. Prediction of lateral form pressure exerted by concrete at low casting rates. *Materials and Structures* 48: 2315–2322.
Poole, J.L., Riding, K.A., Folliard, K.J., Juenger, M. C. G. & Schindler, A. K. 2007. Methods for Calculating Activation Energyfor Portland Cement. *ACI Materials Journal* 104: 303–311.
Reiter, L., Wangler, T., Roussel, N. & Flatt, R.J. 2018. The role of early age structural build-up in digital fabrication with concrete. *Cement and Concrete Research* 112: 86–95.
Roussel, N. 2006. A thixotropy model for fresh fluid concretes: Theory, validation and applications. *Cement and Concrete Research* 36: 1797–1806.
Roussel, N., Ovarlez, G., Garrault, S. & Brumaud, C. 2012. The origins of thixotropy of fresh cement pastes. *Cement and Concrete Research* 42: 148–157.
Watanabe, S. 2018. *Mathematical Theory of Bayesian Statistics* (1st ed.), Chapman and Hall/CRC.